Chapter 13
Small-Molecule Inhibitors of LRRK2

John M. Hatcher, Hwan Geun Choi, Dario R. Alessi, and Nathanael S. Gray

Abstract Mutations in the leucine-rich repeat kinase 2 (LRRK2) protein have been genetically and functionally linked to Parkinson's disease (PD). The kinase activity of LRRK2 is increased by pathogenic mutations; therefore, modulation of LRRK2 kinase activity by a selective small-molecule inhibitor has been proposed as a potentially viable treatment for Parkinson's disease. This chapter presents a historical overview of the development and bioactivity of several small-molecule LRRK2 inhibitors that have been used to inhibit LRRK2 kinase activity in vitro or in vivo. These compounds are important tools for understanding the cellular biology of LRRK2 and for evaluating the potential of LRRK2 inhibitors as disease-modifying PD therapies.

Keywords Parkinson's disease • Leucine-rich repeat kinase 2 (LRRK2) • LRRK2 inhibitors • Mutations

J.M. Hatcher • N.S. Gray (✉)
Department of Cancer Biology, Dana Farber Cancer Institute,
450 Brookline Ave, Boston, MA 02215, USA
e-mail: Johnm_Hatcher@dfci.harvard.edu; nathanael_gray@dfci.harvard.edu

H.G. Choi
New Drug Development Center, Daegu Gyeongbuk Medical Innovation Foundation,
80 Cheombok-ro, Dong-gu, Daegu 41061, South Korea
e-mail: hgchoi@dgmif.re.kr; hwangeun.choi@gmail.com

D.R. Alessi
MRC Protein Phosphorylation and Ubiquitylation Unit, University of Dundee,
Sir James Black Centre, Dow Street, Dundee, DD1 5EH, UK
e-mail: d.r.alessi@dundee.ac.uk

Introduction

Parkinson's disease (PD) is the second most common neurodegenerative disease in the world. It affects over one million Americans and more than 60,000 patients are newly diagnosed each year [1, 2]. Recent genetic studies have revealed an underlying genetic cause in at least 10% of all PD cases [3], which provides new opportunities for the discovery of molecularly targeted therapeutics that may ameliorate neurodegeneration. Among the genes associated with PD, leucine-rich repeat kinase 2 (LRRK2) is unique because a missense mutation, G2019S, is frequently found in both familial and sporadic Parkinson's disease cases [4, 5]. The G2019S mutation increases kinase activity which may result in activation of the neuronal death signal pathway, suggesting that small-molecule LRRK2 kinase inhibitors may be able to serve as a new class of therapeutics for the treatment of Parkinson's disease [6, 7]. Transgenic G2019S LRRK2 mice aged 12–16 months display progressive degeneration of the substantia nigra pars compacta (SNpc) dopaminergic neurons and Parkinson's phenotypes of motor dysfunction suggesting that this mutation may be functionally relevant to the disease [8]. Recent work indicates that LRRK2 directly phosphorylates a subset of the Rab GTPases on an evolutionary conserved residue within the effector interacting-switch II domain [9]. Pathogenic LRRK2 including G2019S mutation increases phosphorylation of endogenous Rabs, and this strongly decreases their affinity to regulatory proteins that bind to the switch II domain including Rab GDP dissociation inhibitors [9]. Given the dearth of potential targets for the treatment of PD and the popularity of kinases as therapeutic targets, it is perhaps not surprising that there has been a very substantial effort to develop potent and selective LRRK2 inhibitors. This chapter presents a historical overview of the development of small-molecule LRRK2 inhibitors from a chemist's perspective.

The first reported LRRK2 inhibitors in 2009 were several ROCK (Rho kinase) inhibitors such as Y-27632 and H-1152, which suppressed LRRK2 with similar potency to which they inhibited ROCK2 as well as sunitinib, a structurally unrelated multikinase inhibitor that suppresses LRRK2, but not ROCK [10]. This study also described for the first time the mutant LRRK2[A2016T] that was normally active but resistant to H-1152, Y-27632, and sunitinib [10]. Prior to the recent identification of Rab GTPase substrates, the effectiveness of inhibitors was assessed by monitoring the dephosphorylation of two phosphorylation sites (Ser910 and Ser935) that mediate binding to 14-3-3 as the phosphorylation of these residues is indirectly controlled by LRRK2 kinase activity through a mechanism that is still not understood [11] (Table 13.1).

Subsequent screening of libraries resulted in compounds that were quite promiscuous kinase inhibitors [12]. A significant advance in the field of small-molecule LRRK2 inhibitors came in 2011 when more selective inhibitors LRRK2-IN-1 (**1**) [13] and CZC-25146 (**2**) [14] were developed through screening of historical kinase inhibitor libraries. LRRK2-IN-1 inhibited both truncated wild-type LRRK2 and LRRK2-G2019S with IC50 values of 13 and 6 nM, respectively, but LRRK2-A2016T and LRRK2-A2016T + G2019S mutants were found to be ~400-fold more

Table 13.1 Early selective LRRK2 inhibitors

1 (LRRK2-IN-1) 2 (CZC-25146) 3 (TAE684)

Compd	MPO score	MW	ClogP	LRRK2 IC50 (nM)[a]	Kinase selectivity	Mouse Cl (mL min^{-1} kg^{-1})[b]	Total B/P[c]
1	4.4	571	2.9	6	12 of 440 < 10% control[d]	5.6	Negligible
2	2.4	489	3.5	7	4 of 184 < 300 nM[e]	2.3	Negligible
3	1.8	614	5.8	6	27 of 440 < 10% control[d]	17	1.7

[a]Biochemical assay; LRRKtide used for compound 1 and Nictide used for compounds 2 and 3; G2019S LRRK2 mutant IC$_{50}$ for compounds 1–3
[b]Compound 1 was dosed i.v. (1 mg kg^{-1}). Compound 2 was dosed i.v. (1 mg kg^{-1}) for both systemic and brain PK. Compound 3 was dosed i.v. (1 mg kg^{-1}) for both systemic and brain PK
[c]Total brain/plasma AUC ratio.
[d]KINOMEscan profiling (1 μM)
[e]Kinobeads profiling (2 μM)

resistant to LRRK2-IN-1. The reason for this resistance was explained using a molecular docking study of LRRK2-IN-1 bound to a homology model of LRRK2-A2016T, which revealed an unfavorable interaction between the anthranilic acid moiety and the A2016T residue. The large degree of resistance conferred by the A2016T mutation provides a convenient method for assessing the degree to which LRRK2-IN-1 observed pharmacology is "on target" to LRRK2 through rescue experiments. LRRK2-IN-1 was moderately selective inhibiting 12 of 440 kinases with <10% activity of control using KINOMEscan profiling. LRRK2-IN-1 induced dose-dependent Ser910 and Ser935 dephosphorylation and loss of 14-3-3 binding to endogenous LRRK2 in human-derived neuroblastoma SHSY5Y cells and Swiss3T3 mouse cells. PK studies of LRRK2-IN-1 showed a half-life of 4.5 h and a bioavailability of 49.4% in mice. However, insufficient blood–brain barrier penetration was found based on evaluation of Ser910 and S935 phosphorylation status in the kidney versus the brain. Subsequent characterization of LRRK2-IN-1 has revealed significant off-target activity on ERK5 [15], DCLK1 [16], and Brd4 (unpublished observations). The activity of LRRK2-IN-1 on Brd4, a general transcriptional coactivator protein [17], confounds the use of LRRK2-IN-1 as a selective LRRK2 inhibitor, and newer compounds described below represent superior pharmacological probes. CZC-25146 inhibited the activity of recombinant human wild-type LRRK2 with an IC50 ranging from 1 to 5 nM. The LRRK2-G2019S mutant was inhibited with an IC50 ranging from 2 to 7 nM in a TF-FRET assay. CZC-21546 was screened against a kinase panel of 184 kinases and only inhibited 4 other kinases with high potency. Additionally, it protects against mutant LRRK2-induced injury of cultured human and rodent neurons with nanomolar potency [14]. Unfortunately, this compound also suffered from poor brain penetration of only 4% [14]. TAE684 (3) [18], which was initially reported as an ALK inhibitor [19], was also found to inhibit LRRK2. It possesses similar structural features as LRRK2-IN-1 and CZC-25146 and displayed similar biochemical potency against LRRK2. TAE684 also inhibits in vivo phosphorylation of mouse Ser910 and Ser935 in the kidney and spleen in a dose-dependent manner following oral administration. Unfortunately, this compound is highly promiscuous inhibitor which binds tightly to 27 of 440 kinases with <10% activity of control.
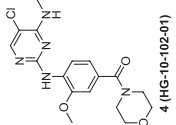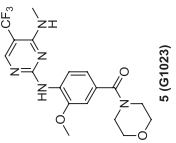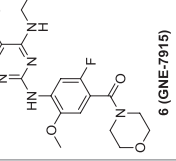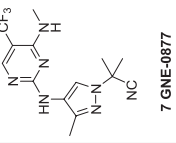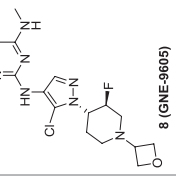
Diaminopyrimidines

The major drawback of compounds **1**–**3** is their inability to probe the effects of LRRK2 inhibition in the CNS. As a result, simplified hybrid structures of **1**, **2**, and **3** were created leading to a variety of lower molecular weight diaminopyrimidines. Compound **4** was reported independently by Gray et al. [20] and Genentech [21] and was found to maintain the ability to potently inhibit the biochemical activity of both wild-type and G2019S mutant LRRK2. Compound **4** exhibited biochemical IC50 values of 20.3 and 3.2 nM against LRRK2-wt and LRRK2-G2019S, respectively. Compound **4** also maintains inhibition of the A2016T mutant due to the

removal of the 4-anilino moiety. Compound **4** was profiled against a panel of 451 kinases using KINOMEscan technology at a concentration of 0.1 μM, which revealed no other interactions except for a mutant form of c-Kit (L576P). The mouse pharmacokinetic profile showed good oral bioavailability (%*F* = 67), a short half-life (0.13 h), and a low plasma exposure [502 h*ng/mL, area under the concentration–time curve $(AUC)_{last}$]. The short half-life was attributed to rapid first-pass metabolism because incubation with mouse liver microsomes revealed a half-life of 13 min. In vivo testing of compound **4** showed LRRK2 inhibition of ~40% at 30 mg/kg and ~70% at 50 and 100 mg/kg in the mouse brain following intraperitoneal administration. An independent medicinal chemical effort by researchers at Genentech resulted in the identification of compound **5** [22]. Compound **5** also featured a high degree of kinase selectivity with no other interactions found in a panel of 178 kinases with >50% inhibition. Compound **5** showed a threefold improvement in the pS1292 cellular assay and an improved in vivo rat PK profile. Compound **5** was used as an in vivo tool to demonstrate the inhibition of in vivo kinase activity in G2019S transgenic mouse brains (pS1292) and the reversal of cellular effects of LRRK2 PD mutations in cultured primary hippocampal neurons. The in vivo unbound brain concentration required to effectively reduce pS1292 autophosphorylation (IC50 = 12 nM) was similar to compound **4**. Additionally, a statistically significant reversal of the neurite outgrowth defects associated with the LRRK2-G2019S mutant [23] was observed upon treatment of LRRK2-G2019S mouse embryonic hippocampal neurons with compound **5** at 100 nM. Compound **5** was screened against a targeted subset of kinases that share a similar ATP-binding site sequence to LRRK2 and showed strong inhibition of TTK. Genentech used the JAK2-based homology model and the TTK cocrystal structures to determine that substitution on the phenyl ring para to the methoxy group would produce steric clash with Asp608 of TTK to increase the selectivity for LRRK2 over TTK. Thus, a few minor structural modifications, including fluorine substitution para to the methoxy group on the phenyl ring position, resulted in the discovery of compound **6** [22]. Compound **6** possessed a nearly identical activity and DMPK profile as compound **5** but with an improved TTK selectivity index (53-fold) and good kinome selectivity at a concentration (0.1 μM) [2/449 kinases with <30% activity of control]. The excellent selectivity profile of optimized inhibitor **6** at 0.1 μM was further established in an Invitrogen kinase selectivity panel [1/197 kinases with >50% inhibition (TTK)].

In an effort to increase the structural diversity and selectivity of the brain-penetrant diaminopyrimidine compounds, Genentech explored aniline bioisosteres, which led to the identification of aminopyrazoles GNE-0877 (**7**) [24] and GNE-9605 (**8**) [24] (Table 13.2) as highly potent and specific LRRK2 inhibitors. Compound **7** was tested in a panel of 188 kinases and showed >50% inhibition of 4 other kinases (Aurora B, RSK2, RSK3, RSK4). Compound **8** inhibited no other kinases to greater than >70% inhibition when tested at a concentration of 1 μM. Compound **8** was tested in a panel of 178 kinases and inhibited one other kinase with >50% inhibition (TAK1-TAB1). Compound **8** inhibited no other kinases with >50% inhibition. Compounds **7** and **8** also showed excellent DMPK profiles (Table 13.3).

Table 13.2 Highly selective aminopyrimidine LRRK2 inhibitors

Structures: 4 (HG-10-102-01), 5 (G1023), 6 (GNE-7915), 7 GNE-0877, 8 (GNE-9605)

Compd	MPO score	MW	ClogP	LRRK2 IC50 (nM)[a]	Kinase selectivity	pLRRK2 IC$_{50}$[b]	Total B/P[c]
4	5.4	378	1.9	3	1 of 451 < 30% of control[d]	29	0.23
5	5.1	411	2.1	2	0 of 178 >50%[e]	9	0.9
6	4.5	443	2.8	1	2 of 449 < 30% of control[d]	9	0.9
7	5.0	339	3.0	0.7	4 of 188 > 50%[e]	3	1.2
8	4.5	450	2.8	2	1 of 178 > 50%[e]	19	0.7

[a]Biochemical assay; LRRKtide and G2019S mutant used for compounds **4–8**
[b]pSer1292 triple mutant (G2019S/R1441G/Y1699C) cellular assay used for compounds **4–8**
[c]Total brain/plasma AUC ratio
[d]KINOMEscan profiling (0.1 μM)
[e]Invitrogen profiling (0.1 μM)

Table 13.3 In vivo and in vitro rat DMPK profiles of diaminopyrimidine LRRK2 inhibitors

Compd	hep Cl_{hep} (mL min^{-1} kg^{-1})[b] h/r[c]	% rat PPB	Cl (Cl_u) (mL min^{-1} kg^{-1})[d]	iv $t_{1/2}$ (h)	%F	MDR1[e] P-gp ER[f] (B:A/A:B)[g]
4	4.9/24	92	51 (616)	0.5	67	2.8
5	1.8/7.6	86	24 (156)	1.2	80	1.2
6	3.2/14	97	8.3 (244)	3.1	40	0.9
7	3/25	79	44 (210)	1.3	90	0.8
8	1/21	79	26 (261)	1.5	90	0.8

[a]Compounds **4**–**8** were dosed p.o. (1 mg kg^{-1}) as an aqueous suspension with 1% methylcellulose, i.v. (0.5 mg kg^{-1}) as a 60% PEG solution or 20–60% NMP solution for systemic PK, and i.v. (0.5 mg kg^{-1}) as a 60% NMP solution for brain PK [21–24]
[b]In vitro stability in cryopreserved hepatocytes
[c]h/r = human/rat
[d]Cl_u = unbound clearance = total clearance/f_{up}, where f_{up} is the unbound plasma free fraction
[e]MDCK-MDR1 human P-gp transfected cell line
[f]Efflux ratio
[g]Basolateral to apical/apical to basolateral

Table 13.4 In vivo NHP PK profiles of Genentech aminopyrimidine LRRK2 inhibitors

Compd	hep Cl_{hep} (mL min^{-1} kg^{-1})[b] NHP	% NHP PPB	Cl (Cl_u) (mL min^{-1} kg^{-1})[c]	iv $t_{1/2}$ (h)	%F	MDR1[d] P-gp ER[e] (BA/A:B)[f]	B_u/P_u[g]	CSF/P_u[h]
6	14	95	11 (200)	7.7	17	0.9	0.6	1.1
7	19	80	20 (100)	2.2	35	0.8	0.7	1.2
8	13	82	8 (43)	4.0	74	0.8	n/a	1.1

[a]Compounds **6**–**8** were dosed p.o. (1 mg kg^{-1}) as an aqueous suspension with 1% methylcellulose and i.v. (0.5 mg kg^{-1}) as a 20–60% NMP solution [22–24]
[b]In vitro stability in cryopreserved hepatocytes
[c]Cl_u = unbound clearance = total clearance/f_{up}, where f_{up} is the unbound plasma free fraction
[d]MDCK-MDR1 human P-gp transfected cell line
[e]Efflux ratio
[f]Basolateral to apical/apical to basolateral
[g]Unbound brain/unbound plasma AUC ratio
[h]CSF/unbound plasma AUC ratio

In vivo nonhuman primate (NHP) PK profiles of compounds **6**, **7**, and **8** are summarized in Table 13.4. All three compounds demonstrated good in vitro–in vivo correlation, moderate plasma clearance rates, and good i.v. half-lives. Additionally, CSF/P ratios extracted from low-dose PK studies suggested that all three compounds possessed approximately equal free brain to free plasma distribution [25]. Desirable B ratios were later confirmed for compounds **7** and **8** during NHP safety assessments (vide infra).

In the absence of a LRRK2-dependent PD efficacy model, in vivo PD knock-down for compounds **6**–**8** was assessed through the use of LRRK2 BAC transgenic mice expressing human LRRK2 protein with the G2019S mutation [23]. Inhibitors were evaluated for their ability to inhibit LRRK2 S1292 autophosphorylation in vivo. Tissue samples were harvested and examined from the hippocampus and

spleen [22]. Dose-dependent inhibition of S1292 phosphorylation was observed for all inhibitors tested in both the brain and peripheral tissues. In vivo unbound brain IC50 values of 7, 3, and 20 nM were calculated for **6**, **7**, and **8**, respectively.

Toxicities Observed with Aminopyrimidine LRRK2 Inhibitors

In 2011, Novartis published a report indicating that lung and kidney abnormalities existed in LRRK2 genetic knockout mice [26]. In order to assess these potential liabilities, Genentech advanced their aminopyrimidine compounds into safety studies. Due to low anti-pS1292 antibody sensitivity, in vivo PD target engagement in all of the studies was assessed using pS935. Male C57BL/6 mice were dosed p.o. with compound **6** (200 and 300 mg kg^{-1} b.i.d.) and compound **7** (30 and 65 mg kg^{-1} b.i.d.) for 15 days. Toxicokinetic analysis showed dose-dependent increases in plasma and brain levels with average free drug exposures of 5- and 36-fold above pS1292 cellular IC50 values for the higher doses. While evidence of lung, kidney, and brain PD knockdown was observed with both inhibitors, no microscopic effects were observed in the lung or kidney, and both compounds were well tolerated. Similar 7-day repeat-dosing studies were conducted in male and female Sprague–Dawley rats. Once daily p.o. administration of compound **6** (10, 50, and 100 mg kg^{-1}) and compound **7** (30, 75, and 200 mg kg^{-1}) showed dose-dependent exposure increases. The highest tolerated doses for compounds **6** (100 mg kg^{-1}) and 7 (30 mg kg^{-1}) translated to maximum free drug exposures of 22- and 195-fold over the cellular IC50 of compound **6** and **7**, respectively. No macroscopic or microscopic effects were seen in the lung or kidney with either compound. Finally, NHPs were dosed orally with compound **6** (10, 25, and 65 mg kg^{-1} q.d.) for 7 days. Toxicokinetic analysis showed a dose-dependent increase in plasma exposures with average free drug levels correlating to 4-, 14-, and 35-fold above the cellular IC50s. Terminal B$_u$/P$_u$ and CSF/P$_u$AUC ratios of 0.6 and 0.8 were achieved, respectively, showing a high degree of brain penetration. Statistically significant PD inhibition of pS935 was observed at all doses tested. Transient and reversible clinical observations included tremors (=10 mg kg^{-1}) and hypoactivity and decreased reactivity to stimulus (25 and 65 mg kg^{-1}). The only anatomic pathology observation linked to compound **6** was limited to the lung and characterized by abnormal cytoplasmic accumulation of secretory lysosome-related organelles known as lamellar bodies in type II pneumocytes of all animals administered 25 and 65 mg kg^{-1} in both sexes. Comparison of these findings with the published LRRK2 knockout mouse data showed that the lung phenotypes were essentially identical. With the goal of examining potential on-target- versus off-target-related effects, structurally distinct aminopyrazole 7 (6 and 20 mg kg^{-1} b.i.d.) and anilinoaminopyrimidine 6 (30 mg kg^{-1} b.i.d.) were administered to NHPs in a 29-day repeat-dose study. Significant free drug coverage above cellular IC50 values and excellent brain penetration were achieved in both tests. PK/PD knockdown of pS935 in the brain, kidney, and lung was confirmed at all doses. Upon microscopic evaluation of the lung, abnormalities identical to those observed in LRRK2 knockout mice were observed at all doses with both inhibitors.

These findings are consistent with an on-target effect of reduction of LRRK2 kinase activity that leads to lamellar body accumulation in type II pneumocytes in the lung of certain species. Interestingly, the morphologic abnormality described for the LRRK2 knockout mouse kidney was absent in both NHP studies.

Arylbenzamides

Researchers at GSK developed a series of arylbenzamides exemplified by GSK2578215A which were reported on in 2012 [27] (**9**, Table 13.5). Compound **9** is a structurally distinct, potent, and highly selective LRRK2 kinase inhibitor that shows inhibition of only 2 other kinases with <10% activity of control (ALK and FLT3) in a panel of 449 kinases. Compound **9** demonstrates moderate mouse plasma clearance (30 mL min^{-1} kg^{-1}), low oral bioavailability (12% at 10 mg/kg), and a total B/P ratio of 1.4 (Table 13.5). In addition, Gray and coworkers were able to demonstrate dose-dependent inhibition of pS910 and pS935 in stably transfected HEK293 cells (wild-type and G2019S LRRK2), with endogenous LRRK2 from lymphoblastoid cells (G2019S PD patient sample) and in mouse Swiss 3T3 cells at approximately 0.3–1.0 μM. In vivo PK/PD analysis of normal mice revealed strong inhibition of pS910 and pS935 in peripheral tissues (spleen and kidney lysates); however, no significant inhibition was detected in the mouse brain despite a total brain to plasma ratio of 1.4. One possible explanation for the lack of brain target engagement could be insufficient free drug levels in the brain relative to the cellular potency. Compound **9** has recently been used to probe the relationship between kinase activity and synaptic vesicle release [28]. Additionally, a patented N-methylpiperazine inhibitor BMPBB-32 [29, 30] (**10**, Table 13.5) closely related to 2-fluoropyridine **9** was profiled. It was reported that piperazine **10** could improve contrast sensitivity in *Drosophila* that overexpress the human LRRK2[G2019S] transgene. Additionally, it was found that N-methylpiperazine benzamide **10** lacks the off-target effects seen with the less selective inhibitor **1** in *Drosophila* in vivo models.

Quinolines and Cinnolines

Elan Pharmaceuticals published their findings on a series of cinnoline [31] and quinoline [32] LRRK2 small-molecule inhibitors, which were identified from a kinase-focused HTS of an in-house library. The screen used a homogeneous time-resolved fluorescence (HTRF) assay measuring the inhibition of phosphorylation of LRRKtide. Hits from this scaffold were known P-gp substrates and inhibitors of PDE4 and CSF1R. Using a MLK1-based homology model, Garofalo and coworkers employed structure-based drug design to develop potent and modestly LRRK2-selective quinolines represented by compound **11** and cinnolines represented by compound **12** (Table 13.6). Quinoline **11** had a biochemical IC50 = 3 nM against

Table 13.5 Arylbenzamide LRRK2 inhibitors

9 (GSK2578215A)

10 (BMPPB-32)

Compd	MPO score	MW	ClogP	LRRK2 IC50 (nM)[a]	Kinase selectivity	pLRRK2 IC50[b]	Cl (mL min⁻¹ kg⁻¹)	iv $t_{1/2}$ (h)	F (%)	Total B/P[c]
9	3.9	399	4.3	9	2 of 449 < 10% of control[e]	n/a	30	1.1	12	1.4
10	4.8	402	3.5	6[d]	3 of 449 < 10% of control[f]	94	n/a	n/a	n/a	0.9

[a]Biochemical assay; Nictide used for compound 9 and LRRKtide used for compound 10; LRRK2 (G2019S) IC$_{50}$ at 100 μM ATP for compounds 9 and 10
[b]pSer935 G2019S mutant cellular assay (HEK293 cells)
[c]Total brain/plasma AUC ratio
[d]LanthaScreen LRRK2 K_i
[e]KINOMEscan profiling (10 μM)
[f]KINOMEscan profiling (1 μM). Compound 9 was dosed p.o. (10 mg kg⁻¹) and i.v. (1 mg kg⁻¹) for both systemic and brain PK.

Table 13.6 Quinoline and cinnoline LRRK2 inhibitors

Compd	MPO score	MW	ClogP	LRRK2 IC50 (nM)[a]	Kinase selectivity	pLRRK2 IC50[b]	Total B/P[c]
11	5.4	291	2.8	3	11 of 39 > 50%[d]	140	1.2
12	4.7	295	2.9	5	n/a	62	1.5

[a]Biochemical assay; LRRKtide used for compound **11** and **12**; LRRK2 (G2019S) IC$_{50}$ at 100 μM ATP
[b]pSer935 G2019S mutant cellular assay (HEK293 cells)
[c]Total brain/plasma AUC ratio
[d]Invitrogen profiling (1 μM)

LRRK2-G2019S and a cellular pS935 EC50 = 140 nM using HEK293 cells stably transfected with LRRK2-G2019S. Quinoline **11** was screened against a panel of 39 kinases and showed inhibition of 11 kinases with >50% inhibition. Guided by the hypothesis that an amide functionality in the original HTS hit was linked to the P-gp-mediated efflux, suitable replacements were discovered, leading to the 3-cyano substitution in **11**, which removed this liability. This also led to a total mouse B/P ratio of 1.2 for quinoline **11** and statistically significant reduction of pS935 in the brains of G2019S LRRK2 transgenic mice at 3 h following oral doses of 30 and 100 mg/kg [31]. Cinnoline **12** had a biochemical IC50 = 5 nM against LRRK2-G2019S and a cellular pS935 EC50 = 62 nM using HEK293 cells stably transfected with LRRK2-G2019S. Cinnoline **12** was found to have a total mouse B/P ratio of 1.5; however, when cinnoline **12** was screened against a panel of 40 kinases, it was found to be highly promiscuous [32].

Triazolopyridazine and Indazole

Elan Pharmaceuticals discovered a series of triazolopyridazines based on a kinase-focused HTS of an in-house library [33]. The screen used a homogeneous time-resolved fluorescence (HTRF) assay measuring the inhibition of phosphorylation of LRRKtide. Based on a homology model built using MLK1, they found that the triazolopyridazines made a single hydrogen bond contact between the triazolo ring and A1950. These compounds displayed a moderate level of selectivity for LRRK2-G2019S over LRRK2-wt with the lead compound **13** having a biochemical IC50 = 76 nM for LRRK2-wt and a biochemical IC50 = 10 nM for LRRK2-G2019S. However, these compounds suffered from oxidative metabolism due to the sulfur linker as well as poor permeability. Pfizer later reported a series of related triazolopyridazines exemplified by compound **14** [34]. This compound was also developed by optimizing a hit from an HTS library screen. Using TYK2 cocrystal structures, they found a single point contact between the kinase hinge (N-H of Val981) and a nitrogen atom of the triazole ring. The absence of hydrogen bond donors in compound **14** is notable, since hydrogen bond donors increase the probability of P-gp recognition and reduce CNS penetration [35]. Through the application of CNS physicochemical property constraints and by use of TYK2 cocrystal structures to facilitate structure-based drug design, compound **14** (Table 13.7) was developed. Triazolopyridazine **14** has a LRRK2-wt IC50 of 64 nM. Compound **14** was screened against a panel of 391 kinases and was found to be highly selective inhibiting only 2 other kinases with <30% of control (TYK2 and JAK3). The in vivo tolerability profile of **14** was assessed in a repeat-dose 14-day PK/PD study in mice at 30 and 300 mg kg^{-1} (n = 5 males/dose). No test article-related findings were reported from the examined tissues, which included microscopic examinations of the lung and kidney. This compound did not show inhibition of pS935 or pS1292 in mouse brains at any dose levels [34].

Table 13.7 Triazolopyridazine and indazole LRRK2 inhibitors

Compd	MPO score	MW	Clog$P$	LRRK2 IC50 (nM)[a]	Kinase selectivity	pLRRK2 IC$_{50}$	Total B/P
				13 (Elan)	**14 (Pfizer)**	**15 MLi-2**	
13	5.4	390	3.5	10	n/a	683[b]	n/a
14	5.6	368	2.7	64	2 of 391 <30% of control[f]	n/a	0.1[d]
15	5.6	379	4.0	0.7	1 of 144 <20% of control[g]	1.4[c]	0.008[e]

[a]Biochemical assay; LRRKtide used for compounds **13**, **14**, and **15**; LRRK2 (G2019S) IC$_{50}$ at 100 μM ATP for compound **13**, LRRK2 (G2019S) IC$_{50}$ at 134 μM ATP for compounds **15**, and LRRK2 (wt) IC50 at 100 μM ATP for compound **14**

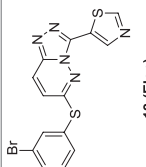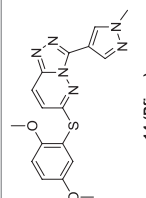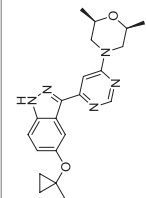[b]pSer935 G2019S mutant cellular assay (HEK293 cells)

[c]pSer935 G2019S mutant cellular assay (SH-SY5Y cells)

[d]Total brain/plasma AUC ratio

[e]Unbound fraction in plasma and brain

[f]KINOMEscan profiling (1 μM)

[g]Dundee profiling (10 μM)

Researchers at Merck recently disclosed the indazole MLi-2 (**15**) [44], a structurally novel, highly potent, and selective LRRK2 kinase inhibitor with central nervous system activity. MLi-2 exhibits exceptional potency in a purified LRRK2 kinase assay in vitro (IC50 = 0.76 nM), a cellular assay monitoring dephosphorylation of LRRK2 pSer935 LRRK2 (IC50 = 1.4 nM), and a radioligand competition binding assay (IC50 53.4 nM). MLi-2 showed inhibition of only 1 other kinase with <20% activity of control in a panel of 144 kinases at a concentration of 10 μM. MLi-2 suppresses LRRK2 Ser935 phosphorylation as well as Rab10 Thr73 phosphorylation at 1–10 nM in mouse embryonic fibroblasts (MEFs) [9]. In mice, a dose of 3 mg/kg of MLi-2 reduces Ser395 phosphorylation as well as Rab8 (Thr72) and Rab12 (Ser105) phosphorylation in the brain to undetectable levels. Treatment of mice with MLi-2 was found to be well tolerated, with no adverse effects of MLi-2 on body weight, food intake, or behavioral activity observed at brain and plasma exposures 100 x the in vivo IC50 for CNS LRRK2 kinase inhibition. Morphologic changes in the lung, consistent with enlarged type II pneumocytes, were observed in MLi-2-treated MitoPark mice. Moreover, the A2016T mutation renders LRRK2 nearly tenfold resistant to MLI-2. Consistent with this, 10 nM MLi-2 induces dephosphorylation of Ser935 and Rab10 (Thr73) in mouse embryonic fibroblasts of wild type but not in LRRK2[A2016T] knockin cells [44]. Furthermore, MLi-2 at 3 mg/kg injected into mice induces complete dephosphorylation of Ser935 in the brain, kidney, lung, and spleen of wild-type mice but not of littermate LRRK2[A2016T] knockin animals (unpublished data).

Indolinones

Sunitinib (**16**) was originally identified as a potent inhibitor of LRRK2; however, high kinase promiscuity precluded the use of this compound for reliable model studies of LRRK2 function. Recently, scientists at Novartis reported the optimization of sunitinib to indolinones **17** [36] and **18** [36] (Table 13.8) with single-digit nanomolar LRRK2 biochemical activity and modest in vivo pharmacokinetic properties. By using an IRAK4-based homology model, the 5-position of the indolinone core was targeted for improving kinase selectivity. This strategy led to the introduction of 5-alkoxy substituents in **16** and **17** that demonstrated improved selectivity profiles over other indolinone-based inhibitors against a small panel of off-target kinases (ALK, KDR, LCK, PDGFRa, and RET). When administered to mice, compound **17** reduced LRRK2 protein levels in the kidney and in the brain. Inhibitor **17**, along with the less selective LRRK2 kinase inhibitor H-1152, was subsequently used by Longo et al. to ameliorate the observed age-dependent hyperkinetic phenotype of LRRK2-G2019S knockin mice [37]. These results suggest that the enhanced kinase activity of the LRRK2[G2019S] protein is responsible for the observed lack of age-related decline in stepping activity and immobility time that was demonstrated by wild type.

Table 13.8 Indolinone LRRK2 inhibitors

Compd	MPO score	MW	ClogP	LRRK2 IC50 (nM)[a]	Kinase selectivity	pLRRK2 IC$_{50}$[b]
	16 (Sunitinib)			**17 (Novartis)**	**18 (Nov-LRRK2-11)**	
16	4.2	398	2.9	19	30 of 140 < 20% of control[c]	370
17	5.1	421	1.6	9	n/a	n/a
18	5.5	365	2.4	4	n/a	380

[a]Biochemical assay IC$_{50}$ at 200 μM ATP for compounds **15–16**
[b]pSer935 cellular assay (NIH3T3 Cells)
[c]Dundee profiling (1 μM)

Pyrrolopyrimidines

The Gray lab reported the discovery of a highly potent and selective brain-penetrant pyrrolopyrimidine LRRK2 inhibitor JH-II-127 (**19**) [38]. This compound was designed based on an intramolecular hydrogen bond between a fluorine of the –CF3 group and the –NHMe group on the pyrimidine of GNE-7915 (**6**) forming a pseudobicycle. Researchers in the Gray lab constructed the ring-closed version to give the pyrrolopyrimidine **19**. They proposed that a fused bicyclic analogue would increase the binding affinity due to the additional third hydrogen bond donor at the 7 position, which is predicted to hydrogen bond with M1949. In addition, they reasoned that a fused bicyclic compound should be able to better fill the hydrophobic area around the hinge region, thus leading to an increase in binding affinity. Their molecular docking study based on the crystal structure of Roco kinase also predicted a sulfur–halogen interaction between the chlorine of the pyrrole ring and the Met1947 residue. Compound **19** had a biochemical IC50 of 6.6 nM against LRRK2-wt and 2.2 nM against LRRK2-G2019S. Compound **19** induced a dose-dependent inhibition of Ser910 and Ser935 phosphorylation in both wild-type LRRK2 and LRRK2-G2019S stably transfected into HEK293 cells. Substantial dephosphorylation of Ser910 and Ser935 was observed at approximately 0.3 μM concentrations of **19** for wild-type LRRK2 and LRRK2-G2019S, which is a similar potency to that observed for LRRK2-IN-1 (**1**). Consistent with the biochemical results, **19** also induced dephosphorylation of Ser910 and Ser935 at a concentration of 0.3─1 μM in the drug-resistant LRRK2[A2016T + G2019S] and LRRK2[A2016T] mutants, revealing that the A2016T mutation does not induce resistance to **19**. Compound **19** was tested on endogenously expressed LRRK2 in human lymphoblastoid cells derived from a control and Parkinson's patient homozygous for the LRRK2-G2019S mutation. Increasing doses of **19** led to similar dephosphorylation of endogenous LRRK2 at Ser910 and Ser935, as was observed in HEK293 cells stably expressing wild-type LRRK2 or LRRK2-G2019S. Moreover, endogenous LRRK2 was also more sensitive to **19** than LRRK2-IN-1 (**1**), which is consistent with the trend observed in HEK293 cells. It was also found that **19** induced similar dose-dependent Ser935 dephosphorylation of endogenous LRRK2 in mouse Swiss 3T3 cells. The mouse pharmacokinetic profile of **19** demonstrated good oral bioavailability (116 %*F*), a half-life of 0.66 h, and a plasma exposure of 3094 (hr * ng/mL, AUC$_{last}$) following 10 mg/kg p.o. dosing (Table 13.9). Additionally, following 2 mg/kg i.v. dosing, **19** showed a plasma exposure of 533 (hr * ng/mL, AUC$_{last}$) and a brain exposure of 239 (hr * ng/mL, AUC$_{last}$), which equates to a brain/plasma concentration ratio of 0.45. They compared the pharmacodynamic properties of **19** with GNE-7915 (**6**) by monitoring inhibition of LRRK2 Ser910/Ser935 phosphorylation in the kidney, spleen, and brain following intraperitoneal delivery of each compound at 100 mg/kg. They observed near-complete dephosphorylation of Ser935 of LRRK2 in all tissues including the brain at this dose for both compounds. They repeated the study at lower doses of 50, 30, and 10 mg/kg of **19** and **6**. With **19**, they observed near-complete inhibition in all tissues at 30 mg/kg but only partial

**Table 13.9** Pyrrolopyrimidine LRRK2 inhibitors

Compd	MPO score	MW	ClogP	LRRK2 IC50 (nM)[a]	Kinase selectivity	pLRRK2 IC$_{50}$[b]	Cl (mL min^{-1} kg^{-1})	iv $t_{1/2}$ (h)	F (%)	Total B/P[c]
19	4.8	416	3.3	2	2 of 451 < 10% of control[d]	7	62	1.1	116	0.45
20	5.7	305	2.2	11	3 of 449 < 30% of control[d]	25	n/a	n/a	n/a	0.9

19 (JH-II-127)

20 (PF-06447475)

[a]Biochemical assay; Nictide used for compound **19**. LRRKtide used for compound **20**; LRRK2 (G2019S) IC$_{50}$ at 100 μM ATP for compound **19** and LRRK2 (G2019S) IC$_{50}$ at 50 μM ATP for compound **20**
[b]pSer935 G2019S mutant cellular assay (HEK293 cells)
[c]Total brain/plasma AUC ratio
[d]KINOMEscan profiling (1 μM)
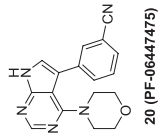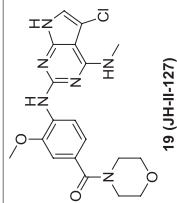
inhibition in the brain at the 10 mg/kg dose. However, with **6**, complete inhibition in the brain was only observed at the 100 mg/kg. These results indicate that **19** is a promising chemo-type for achieving dephosphorylation of Ser935 in the brain. KINOMEscan analysis against a near comprehensive panel of 451 kinases at a concentration of 1 μM resulted in no interactions with kinases other than LRRK2[G2019S] with the exception of TTK and RPS6KA4 [38].

Pfizer reported the identification of a pyrrolopyrimidine scaffold that provided a highly efficient starting point with favorable CNS properties for lead optimization. Using MST3 as a crystallographic surrogate for LRRK2 (reported MST3-LRRK2 ATP-binding site residue similarity of 73%), they improved the off-target liabilities of early HTS leads. This led to the discovery of PF-06447475 (**20**, Table 13.9) [39] with in vitro LRRK2-wt and LRRK2-G2019S biochemical IC50 values of 3 and 11 nM, respectively, and a pS935 cellular IC50 of 25 nM. KINOMEscan profiling of 449 kinases at 1 μM showed inhibition of 3 kinases with <30% activity of control. Selectivity profiling of pyrrolopyrimidine **20** in a cellular context was performed using the ActivX KiNativ technology demonstrating good selectivity in human peripheral blood mononuclear cells at 1 μM and an ActivX LRRK2 cellular IC of 15 nM. Compound **20** is not a P-gp substrate and has moderate and high turnover in human and rat liver microsomes, respectively. The oral in vivo PK profile for **20** in rat, dog, and NHP was also determined. While low oral exposure in higher species precluded further clinical advancement, sufficient oral bioavailability in rodents was achieved, which enabled in vivo mouse PK/PD studies. Additionally, inhibitor **20** exhibited approximate equal distribution of free drug between the rat brain, plasma, and kidney tissues. Dose-dependent reduction in phosphorylation in the brain and kidney was observed in wild-type and G2019S BAC transgenic mice [39]. From these experiments, in vivo unbound brain EC values of 8 nM LRRK2-wt and 103 nM LRRK2-G2019S were calculated using the pS935 biomarker, and 21 nM (G2019S) was calculated for pS1292. On the basis of a clean in vitro safety profile (Ames, MNT, THLE cell viability), pyrrolopyrimidine **20** was evaluated in a 14-day repeat-dose rat toxicity study (3, 10, and 30 mg kg^{-1} b.i.d.). No major test article-related findings were observed with day 11 maximum free drug exposures 6-, 25-, and 70-fold over the cellular EC (15 nM), respectively. Similar to the rat toxicity studies carried out with Genentech aminopyrimidines, no changes were noted upon close examination of the kidney and lung tissue.

Docking Studies

Molecular docking studies were recently conducted by our lab on representative classes of LRRK2 inhibitors, including HG-10-102-01 (**4**), JH-II-127 (**19**), GSK2578215A (**9**), and compound **13** (Elan), based on a crystal structure of Roco kinase (PDB accession code: 4F1T). These studies predicted two hydrogen bonds between the hinge region A1950 and the aminopyrimidine motif of HG-2-102-01 (**4**) as well as a sulfur–halogen interaction between the 5-chloro substituent on the pyrimidine ring and M1947 (Fig. 13.1a). The docking model of JH-II-127 (**19**) predicted the same two hydrogen bonds between the hinge region A1950 and the
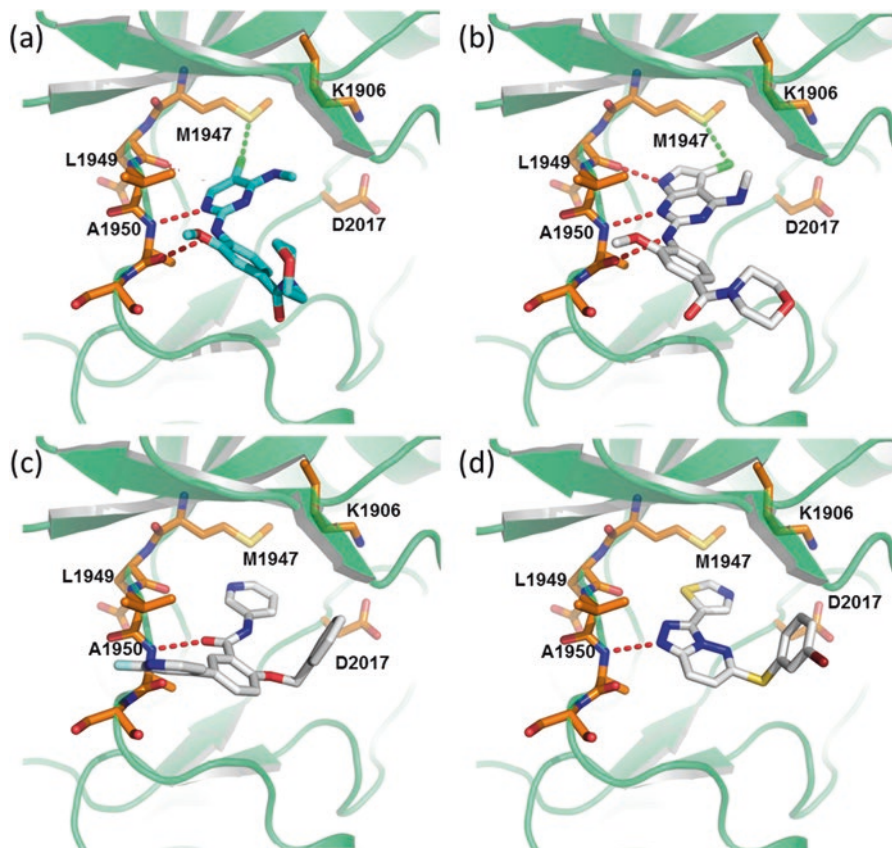
Fig. 13.1 Molecular model of HG-10-102-01 (**a**), JH-II-127 (**b**), GSK2578215A (**c**), and compound **13** from Elan (**d**)

aminopyrrolopyrimidine motif and the sulfur–halogen interaction between the 5-chloro substituent on the pyrrolopyrimidine ring and M1947; however, the docking study also predicted an additional hydrogen bond between the –NH of the pyrrolopyrimidine ring and the carbonyl group of L1949 (Fig. 13.1b). Surprisingly, the docking study for both GSK2578215A (**9**) and compound **13** (Elan) predicted only a single hydrogen bond between the hinge region A1950 and the carbonyl group of GSK2578215A (Fig. 13.1c) and the –N- of the triazolopyridazine of compound **13** (Elan) (Fig. 13.1d).

LRRK2 GTP-Binding Inhibitors

Li et al. recently discovered a series of novel LRRK2 GTP-binding inhibitors **20** and **21** (Fig. 13.2) [40] through virtual screening using an LRRK2 GTPase ROC domain crystal structure (PDB code 2zej) [41]. Both compounds demonstrate in vitro LRRK2

Fig. 13.2 LRRK2
GTP-binding inhibitors
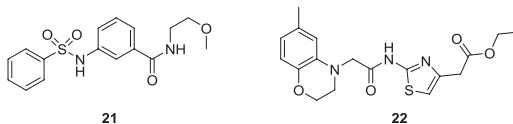
GTP-binding and kinase inhibitory activities in the nanomolar range. Inhibitors **21** and **22** also inhibited LRRK2-induced neuronal degeneration in SH-SY5Y cells and mouse primary cortical neurons at nanomolar concentrations. Compound **21** was selected for in vivo studies using G2019S BAC transgenic mice due to a better solubility profile. At 1 h after i.p. injection of 20 mg/kg, reduction of LRRK2 GTP-binding activity and LRRK2 phosphorylation in mouse brains was observed, indicating CNS penetration. Based on a recent study that found increases in LRRK2 expression and kinase activity following lipopolysaccharide (LPS) stimulation [42, 43], they examined the effects of compound **21** in G2019S BAC transgenic mice following LPS injection. Reduction in LPS-induced microglia activation, LRRK2 expression, and LRRK2 phosphorylation in activated microglia cells was observed. These studies support a potentially promising and orthogonal approach, compared to ATP kinase inhibitors for the use of LRRK2 GTP inhibitors in LRRK2-associated PD.

Conclusions

LRRK2 was found to be linked to PD in several studies and by the examination of families with high incidence of disease. Over the past decade, researchers have been working to advance our understanding of LRRK2 protein and its function. Several structurally diverse inhibitors of LRRK2 function have been discovered, which can be used to monitor LRRK2 in vivo. Given the significant expense and complexity of clinical studies assessing inhibitors of neurodegeneration, a more complete understanding of the cellular function of LRRK2 will most likely be required before studies can be performed to assess the clinical utility of LRRK2 inhibitors.

Although initially it seemed that LRRK2-focused genetic manipulation of rodents would cause accumulation of deficits that resemble PD with age, these animals have exhibited fairly subtle and variable phenotypes. Only recently has a selective LRRK2 kinase inhibitor been reported to modulate some of these deficits. More importantly, LRRK2 knockout rodents and the LRRK2 kinase-dead knockin mice display unusual lung and/or kidney pathology. While several LRRK2 kinase inhibitors have been well tolerated in rats, two molecules have been found to be associated with lung toxicities in NHPs that are histopathologically identical to the LRRK2 knockout rodent phenotype, suggesting an LRRK2-related effect. There is some uncertainty surrounding the clinical consequences of this type II pneumocyte lamellar body accumulation in the lungs of patients, and pulmonary toxicities are challenging to monitor in the clinic. These findings indicate the need for mutant-selective LRRK2 inhibitors, which may not cause the accumulation of lamellar bodies.

Further examination of the toxicities associated with structurally diverse LRRK2 inhibitors in higher species will permit a more complete assessment of the risks of inhibiting LRRK2 kinase activity in man; however, a large degree of uncertainty regarding the therapeutic index of LRRK2 inhibitors is likely to remain due to the absence of direct biomarkers of LRRK2 function and the lack of suitable efficacy models.

To study the impact of inhibiting LRRK2, we would strongly recommend the use of MLi-2 inhibitor which is the most selective or potent in conjunction with one of the other highly characterized structurally diverse LRRK2 inhibitors such as **19** and **20**. In addition we would strongly advocate where possible to combine the power or pharmacological and genetic approaches by exploiting inhibitor-resistant LRRK2[A2016T] knockin cells or mice model. As the A2016T mutation renders LRRK2 ~10-fold resistant to MLi-2 [44], genuine effects that are mediated through inhibition of LRRK2 would be suppressed at a ~10-fold lower dose in wild-type compared to LRRK2[A2016T] mice or cells.

From a kinase inhibitor pharmacology perspective, LRRK2 is amenable to inhibition by a surprisingly diverse array of structurally distinct ATP-competitive inhibitors. In addition, these LRRK2 inhibitors are among the most selective and "drug-like" inhibitors reported for any kinase. To date no LRRK2 kinase structures have been solved, but eventually acquisition of such structures will provide a means to rationalize the remarkable kinase selectivity achieved by some of these inhibitors.

Conflict of Interest The author declares no conflicts of interest.

References

1. Gandhi PN, Chen SG, Wilson-Delfosse AL (2009) Leucine-rich repeat kinase 2 (LRRK2): a key player in the pathogenesis of Parkinson's disease. J Neurosci Res 87(6):1283–1295
2. Dorsey ER, Constantinescu R, Thompson JP, Biglan KM, Holloway RG, Kieburtz K, Marshall FJ, Ravina BM, Schifitto G, Siderowf A, Tanner CM (2007) Projected number of people with Parkinson disease in the most populous nations, 2005 through 2030. Neurology 68(5):384–386
3. Daniëls V, Baekelandt V, Taymans JM (2011) On the road to Leucine-Rich repeat Kinase 2 signalling: evidence from cellular and in vivo studies. Neurosignals 19(1):1–15
4. Healy DG, Falchi M, O'Sullivan SS, Bonifati V, Durr A, Bressman S, Brice A, Aasly J, Zabetian CP, Goldwurm S, Ferreira JJ, Tolosa E, Kay DM, Klein C, Williams DR, Marras C, Lang AE, Wszolek ZK, Berciano J, Schapira AHV, Lynch T, Bhatia KP, Gasser T, Lees AJ, Wood NW (2008) Phenotype, genotype, and worldwide genetic penetrance of LRRK2-associated Parkinson's disease: a case–control study. Lancet Neurol 7(7):583–590
5. Dachsel JC, Farrer MJ (2010) LRRK2 and Parkinson disease. Arch Neurol 67(5):542–547
6. Greggio E, Cookson MR (2009) Leucine-rich repeat kinase 2 mutations and Parkinson's disease: three questions. ASN Neuro 1(1), e00002
7. Kumar A, Cookson MR (2011) Role of LRRK2 kinase dysfunction in Parkinson disease. Expert Rev Mol Med 13:e20. doi: 10.1017/S146239941100192X

8. Chen CY, Weng YH, Chien KY, Lin KJ, Yeh TH, Cheng YP, Lu CS, Wang HL (2012) (G2019S) LRRK2 activates MKK4-JNK pathway and causes degeneration of SN dopaminergic neurons in a transgenic mouse model of PD. Cell Death Differ 19(10):1623–1633

9. Steger M, Tonelli F, Ito G, Davies P, Trost M, Vetter M, Wachter S, Lorentzen E, Duddy G, Wilson S, Baptista M, Fiske B, Fell M, Morrow J, Reith A, Alessi D, Mann M (2016) Phosphoproteomics reveals that Parkinson's disease kinase LRRK2 regulates a subset of Rab GTPases. Elife 10:12813

10. Nichols RJ, Dzamko N, Hutti JE, Cantley LC, Deak M, Moran J, Bamborough P, Reith AD, Alessi DR (2009) Substrate specificity and inhibitors of LRRK2, a protein kinase mutated in Parkinson's disease. Biochem J 424:47–60

11. Dzamko N, Deak M, Hentati F, Reith AD, Prescott AR, Alessi DR, Nichols RJ (2010) Inhibition of LRRK2 kinase activity leads to dephosphorylation of Ser(910)/Ser(935), disruption of 14-3-3 binding and altered cytoplasmic localization. Biochem J 430:405–413

12. Kramer T, Lo Monte F, Goring S, Amombo GMO, Schmidt B (2012) Small molecule kinase inhibitors for LRRK2 and their application to Parkinson's disease models. ACS Chem Nerosci 3(3):151–160

13. Deng XM, Dzamko N, Prescott A, Davies P, Liu QS, Yang QK, Lee JD, Patricelli MP, Nomanbhoy TK, Alessi DR, Gray NS (2011) Characterization of a selective inhibitor of the Parkinson's disease kinase LRRK2. Nat Chem Biol 7(4):203–205

14. Ramsden N, Perrin J, Ren Z, Lee BD, Zinn N, Dawson VL, Tam D, Bova M, Lang M, Drewes G, Bantscheff M, Bard F, Dawson TM, Hopf C (2011) Chemoproteomics-based design of potent LRRK2-selective lead compounds that attenuate Parkinson's disease-related toxicity in human neurons. ACS Chem Biol 6(10):1021–1028

15. Deng XM, Elkins JM, Zhang JW, Yang QK, Erazo T, Gomez N, Choi HG, Wang JH, Dzamko N, Lee JD, Sim T, Kim N, Alessi DR, Lizcano JM, Knapp S, Gray NS (2013) Structural determinants for ERK5 (MAPK7) and leucine rich repeat kinase 2 activities of benzo e pyrimido-5,4-b diazepine-6(11H)-ones. Eur J Med Chem 70:758–767

16. Weygant N, Qu DF, Berry WL, May R, Chandrakesan P, Owen DB, Sureban SM, Ali N, Janknecht R, Houchen CW (2014) Small molecule kinase inhibitor LRRK2-IN-1 demonstrates potent activity against colorectal and pancreatic cancer through inhibition of doublecortin-like kinase 1. Mol Cancer 13:14

17. Fu LL, Tian M, Li X, Li JJ, Huang J, Ouyang L, Zhang YH, Liu B (2015) Inhibition of BET bromodomains as a therapeutic strategy for cancer drug discovery. Oncotarget 6(8):5501–5516

18. Zhang JW, Deng XM, Choi HG, Alessi DR, Gray NS (2012) Characterization of TAE684 as a potent LRRK2 kinase inhibitor. Bioorg Med Chem Lett 22(5):1864–1869

19. Galkin AV, Melnick JS, Kim S, Hood TL, Li NX, Li LT, Xia G, Steensma R, Chopiuk G, Jiang JQ, Wan YQ, Ding P, Liu Y, Sun FX, Schultz PG, Gray NS, Warmuth M (2007) Identification of NVP-TAE684, a potent, selective, and efficacious inhibitor of NPM-ALK. Proc Natl Acad Sci U S A 104(1):270–275

20. Choi HG, Zhang JW, Deng XM, Hatcher JM, Patricelli MP, Zhao Z, Alessi DR, Gray NS (2012) Brain penetrant LRRK2 inhibitor. ACS Med Chem Lett 3(8):658–662

21. Chen HF, Chan BK, Drummond J, Estrada AA, Gunzner-Toste J, Liu XR, Liu YC, Moffat J, Shore D, Sweeney ZK, Tran T, Wang SM, Zhao GL, Zhu HT, Burdick DJ (2012) Discovery of selective LRRK2 inhibitors guided by computational analysis and molecular modeling. J Med Chem 55(11):5536–5545

22. Estrada AA, Liu XR, Baker-Glenn C, Beresford A, Burdick DJ, Chambers M, Chan BK, Chen HF, Ding X, Di Pasquale AG, Dominguez SL, Dotson J, Drummond J, Flagella M, Flynn S, Fuji R, Gill A, Gunzner-Toste J, Harris SF, Heffron TP, Kleinheinz T, Lee DW, Le Pichon CE, Lyssikatos JP, Medhurst AD, Moffat JG, Mukund S, Nash K, Scearce-Levie K, Sheng ZJ, Shore DG, Tran T, Trivedi N, Wang SM, Zhang S, Zhang XL, Zhao GL, Zhu HT, Sweeney ZK (2012) Discovery of highly potent, selective, and brain-penetrable leucine-rich repeat kinase 2 (LRRK) small molecule inhibitors. J Med Chem 55(22):9416–9433

23. Sheng ZJ, Zhang SO, Bustos D, Kleinheinz T, Le Pichon CE, Dominguez SL, Solanoy HO, Drummond J, Zhang XL, Ding X, Cai F, Song QH, Li XT, Yue ZY, van der Brug MP, Burdick DJ, Gunzner-Toste J, Chen HF, Liu XR, Estrada AA, Sweeney ZK, Scearce-Levie K, Moffat JG, Kirkpatrick DS, Zhu HT (2012) Ser(1292) autophosphorylation is an indicator of LRRK2 kinase activity and contributes to the cellular effects of PD mutations. Sci Transl Med 4(164):12

24. Estrada AA, Chan BK, Baker-Glenn C, Beresford A, Burdick DJ, Chambers M, Chen HF, Dominguez SL, Dotson J, Drummond J, Flagella M, Fuji R, Gill A, Halladay J, Harris SF, Heffron TP, Kleinheinz T, Lee DW, Le Pichon CE, Liu XR, Lyssikatos JP, Medhurst AD, Moffat JG, Nash K, Scearce-Levie K, Sheng ZJ, Shore DG, Wong S, Zhang S, Zhang XL, Zhu HT, Sweeney ZK (2014) Discovery of highly potent, selective, and brain-penetrant aminopyrazole leucine-rich repeat kinase 2 (LRRK2) small molecule inhibitors. J Med Chem 57(3):921–936

25. (a) Liu XR, Smith BJ, Chen C, Callegari E, Becker SL, Chen X, Cianfrogna J, Doran AC, Doran SD, Gibbs JP, Hosea N, Liu JH, Nelson FR, Szewc MA, Van Deusen J (2006) Evaluation of cerebrospinal fluid concentration and plasma free concentration as a surrogate measurement for brain free concentration. Drug Metab Dispos 34(9):1443–1447; (b) Lin JH (2008) CSF as a surrogate for assessing CNS exposure: an industrial perspective. Curr Drug Metab 9(1):46–59

26. Herzig MC, Kolly C, Persohn E, Theil D, Schweizer T, Hafner T, Stemmelen C, Troxler TJ, Schmid P, Danner S, Schnell CR, Mueller M, Kinzel B, Grevot A, Bolognani F, Stirn M, Kuhn RR, Kaupmann K, van der Putten PH, Rovelli G, Shimshek DR (2011) LRRK2 protein levels are determined by kinase function and are crucial for kidney and lung homeostasis in mice. Hum Mol Genet 20(21):4209–4223

27. Reith AD, Bamborough P, Jandu K, Andreotti D, Mensah L, Dossang P, Choi HG, Deng XM, Zhang JW, Alessi DR, Gray NS (2012) GSK2578215A; a potent and highly selective 2-arylmethyloxy-5-substitutent-N-arylbenzamide LRRK2 kinase inhibitor. Bioorg Med Chem Lett 22(17):5625–5629

28. Cirnaru MD, Marte A, Belluzzi E, Russo I, Gabrielli M, Longo F, Arcuri L, Murru L, Bubacco L, Matteoli M, Fedele E, Sala C, Passafaro M, Morari M, Greggio E, Onofri F, Piccoli G (2014) LRRK2 kinase activity regulates synaptic vesicle trafficking and neurotransmitter release through modulation of LRRK2 macro-molecular complex. Front Mol Neurosci 7:12

29. Nichols PL, Eatherton AJ, Bamborough P, Jandu KS, Philps OJ, Andreotti D (2011) Novel compounds. Google Patents WO 2011038572 A1, 27 Sept 2010

30. Afsari F, Christensen KV, Smith GP, Hentzer M, Nippe OM, Elliott CJH, Wade AR (2014) Abnormal visual gain control in a Parkinson's disease model. Hum Mol Genet 23(17):4465–4478

31. Garofalo AW, Adler M, Aubele DL, Bowers S, Franzini M, Goldbach E, Lorentzen C, Neitz RJ, Probst GD, Quinn KP, Santiago P, Sham HL, Tam D, Truong AP, Ye XCM, Ren Z (2013) Novel cinnoline-based inhibitors of LRRK2 kinase activity. Bioorg Med Chem Lett 23(1):71–74

32. Garofalo AW, Adler M, Aubele DL, Brigham EF, Chian D, Franzini M, Goldbach E, Kwong GT, Motter R, Probst GD, Quinn KP, Ruslim L, Sham HL, Tam D, Tanaka P, Truong AP, Ye XCM, Ren Z (2013) Discovery of 4-alkylamino-7-aryl-3-cyanoquinoline LRRK2 kinase inhibitors. Bioorg Med Chem Lett 23(7):1974–1977

33. Franzini M, Ye XCM, Adler M, Aubele DL, Garofalo AW, Gauby S, Goldbach E, Probst GD, Quinn KP, Santiago P, Sham HL, Tam D, Truong A, Ren Z (2013) Triazolopyridazine LRRK2 kinase inhibitors. Bioorg Med Chem Lett 23(7):1967–1973

34. Galatsis P, Henderson JL, Kormos BL, Han S, Kurumbail RG, Wager TT, Verhoest PR, Noell GS, Chen Y, Needle E, Berger Z, Steyn SJ, Houle C, Hirst WD (2014) Kinase domain inhibition of leucine rich repeat kinase 2 (LRRK2) using a 1,2,4 triazolo 4,3-b pyridazine scaffold. Bioorg Med Chem Lett 24(17):4132–4140

35. Rankovic Z (2015) CNS drug design: balancing physicochemical properties for optimal brain exposure. J Med Chem 58(6):2584–2608

36. Troxler T, Greenidge P, Zimmermann K, Desrayaud S, Druckes P, Schweizer T, Stauffer D, Rovelli G, Shimshek DR (2013) Discovery of novel indolinone-based, potent, selective and brain penetrant inhibitors of LRRK2. Bioorg Med Chem Lett 23(14):4085–4090

37. Longo F, Russo I, Shimshek DR, Greggio E, Morari M (2014) Genetic and pharmacological evidence that G2019S LRRK2 confers a hyperkinetic phenotype, resistant to motor decline associated with aging. Neurobiol Dis 71:62–73

38. Hatcher JM, Zhang JW, Choi HG, Ito G, Alessi DR, Gray NS (2015) Discovery of a pyrrolopy-rimidine (JH-II-127), a highly potent, selective, and brain penetrant LRRK2 inhibitor. ACS Med Chem Lett 6(5):584–589

39. Henderson JL, Kormos BL, Hayward MM, Coffman KJ, Jasti J, Kurumbail RG, Wager TT, Verhoest PR, Noell GS, Chen Y, Needle E, Berger Z, Steyn SJ, Houle C, Hirst WD, Galatsis P (2015) Discovery and preclinical profiling of 3–4-(Morpholin-4-yl)-7H-pyrrolo 2,3-d pyrimidin-5-yl benzonitrile (PF-06447475), a highly potent, selective, brain penetrant, and in vivo active LRRK2 kinase inhibitor. J Med Chem 58(1):419–432

40. Li TX, Yang DJ, Zhong SJ, Thomas JM, Xue FT, Liu JN, Kong LB, Voulalas P, Hassan HE, Park JS, MacKerell AD, Smith WW (2014) Novel LRRK2 GTP-binding inhibitors reduced degeneration in Parkinson's disease cell and mouse models. Hum Mol Genet 23(23): 6212–6222

41. Deng JP, Lewis PA, Greggio E, Sluch E, Beilina A, Cookson MR (2008) Structure of the ROC domain from the Parkinson's disease-associated leucine-rich repeat kinase 2 reveals a dimeric GTPase. Proc Natl Acad Sci U S A 105(5):1499–1504

42. Moehle MS, Webber PJ, Tse T, Sukar N, Standaert DG, DeSilva TM, Cowell RM, West AB (2012) LRRK2 inhibition attenuates microglial inflammatory responses. J Neurosci 32(5):1602–1611

43. Gardet A, Benita Y, Li C, Sands BE, Ballester I, Stevens C, Korzenik JR, Rioux JD, Daly MJ, Xavier RJ, Podolsky DK (2010) LRRK2 is involved in the IFN-gamma response and host response to pathogens. J Immunol 185(9):5577–5585

44. Fell MJ, Mirescu C, Basu K, Cheewatrakoolpong B, DeMong DE, Ellis JM, Hyde LA, Lin YH, Markgraf CG, Mei H, Miller M, Poulet FM, Scott JD, Smith MD, Yin ZZ, Zhou XP, Parker EM, Kennedy ME, Morrow JA (2015) MLi-2, a potent, selective, and centrally active compound for exploring the therapeutic potential and safety of LRRK2 kinase inhibitions. J Pharmacol Exp Ther 355(3):397–409